nature neuroscience

Slow oscillations in two pairs of dopaminergic neurons gate long-term memory formation in *Drosophila*

Pierre-Yves Plaçais[1,6], Séverine Trannoy[1,6], Guillaume Isabel[1,5,6], Yoshinori Aso[2,5], Igor Siwanowicz[2], Ghislain Belliart-Guérin[1], Philippe Vernier[3], Serge Birman[4], Hiromu Tanimoto[2] & Thomas Preat[1]

A fundamental duty of any efficient memory system is to prevent long-lasting storage of poorly relevant information. However, little is known about dedicated mechanisms that appropriately trigger production of long-term memory (LTM). We examined the role of *Drosophila* dopaminergic neurons in the control of LTM formation and found that they act as a switch between two exclusive consolidation pathways leading to LTM or anesthesia-resistant memory (ARM). Blockade, after aversive olfactory conditioning, of three pairs of dopaminergic neurons projecting on mushroom bodies, the olfactory memory center, enhanced ARM, whereas their overactivation conversely impaired ARM. Notably, blockade of these neurons during the intertrial intervals of a spaced training precluded LTM formation. Two pairs of these dopaminergic neurons displayed sustained calcium oscillations in naive flies. Oscillations were weakened by ARM-inducing massed training and were enhanced during LTM formation. Our results indicate that oscillations of two pairs of dopaminergic neurons control ARM levels and gate LTM.

Abilities of indiscriminate remembering, which, for example, occur with disproportionate frequency in autistic individuals[1], betray brain injury or functional disorders[1,2]. However, little is known about the dedicated mechanisms that trigger the consolidation of memory traces into LTM only for relevant learned experiences. In *Drosophila*, in the context of aversive olfactory learning, two different types of consolidated memory have been characterized[3]: LTM, which relies on *de novo* protein synthesis, and ARM, which does not. We previously proposed that these two memory phases were mutually exclusive[4]; the engagement into the ARM pathway thus preventing the energetically costly[5] formation of LTM when it is not necessary. However, whether ARM and LTM actually antagonize each other has been debated[6], and the putative role of ARM inhibition during LTM formation remains unknown.

In mammals, dopamine, a neuromodulator involved in reward learning[7], intervenes shortly after conditioning[8,9] or as late as 12 h after conditioning[10] in the maintenance of LTM. However, the physiological processes at work in dopaminergic neurons during memory consolidation remain unclear. In *Drosophila*, dopamine is involved in a broad range of behavioral functions[11,12]. In the framework of aversive olfactory memory resulting from simultaneous exposure to electric shocks and an odorant[3,13,14], efforts have focused on the role of dopaminergic neurons in learning[15–17], leaving a putative function of dopaminergic neurons in memory consolidation mostly unexplored. A single study has reported that dopaminergic neurons are involved in the memory impairment induced by heat stress after conditioning[18].

Three bilateral clusters of dopaminergic neurons (PAM, PPL1 and PPL2ab, amounting to ~200, 24 and 12 dopaminergic neurons, respectively, out of ~280 total in the protocerebrum[19]) were identified as projecting to the mushroom bodies, paired multilobed structures that are the essential memory centers[20], and were classified according to the mushroom body region that they innervate[17,21].

We found that blockade, via the expression of a thermosensitive *Shibire* mutant protein[22,23], or overactivation, via the thermosensitive channel *TrpA1* (refs. 17,23), of three pairs of PPL1 dopaminergic neurons enhanced or inhibited, respectively, ARM consolidation. We characterized a sustained oscillatory activity of two pairs of these neurons by *in vivo* imaging in naive flies, and we found that these oscillations correlated with ARM inhibition in trained flies. In addition, we found that the pathways leading to ARM and LTM are exclusive and, consequently, that the ARM-regulating PPL1 dopaminergic neurons are endowed with the ability to gate the formation of LTM during the intertrial intervals (ITIs) of spaced conditioning.

RESULTS

Dopaminergic neurons regulate ARM

We began with the tyrosine hydroxylase (*Th*, also known as *ple*)-*GAL4* fly line[24], which extensively labels most dopaminergic neurons clusters, including the PPL1 and PPL2ab clusters, except the PAM cluster, which is sparsely labeled[16,19,24]. The *Th-GAL4* driver was used in combination with *UAS-shi^{ts}* or *UAS-TrpA1* to transiently block or stimulate, respectively, brain dopaminergic neurons after conditioning.

[1]Genes and Dynamics of Memory Systems, Neurobiology Unit, Centre National de la Recherche Scientifique, École Supérieure de Physique et de Chimie Industrielles (ESPCI), Paris, France. [2]Behavioral Genetics, Max Planck Institute of Neurobiology, Martinsried, Germany. [3]Développement, Evolution, Plasticité du Système Nerveux, Institut de Neurobiologie Alfred-Fessard, Centre National de la Recherche Scientifique, Gif-sur-Yvette, France. [4]Genetics and Physiopathology of Neurotransmission, Neurobiology Unit, Centre National de la Recherche Scientifique, ESPCI, Paris, France. [5]Present addresses: Centre de Recherches sur la Cognition Animale, Université Paul Sabatier, Toulouse, France (G.I.) and Janelia Farm Research Campus, Howard Hughes Medical Institute, Ashburn, Virginia, USA (Y.A.). [6]These authors contributed equally to this work. Correspondence should be addressed to T.P. (thomas.preat@espci.fr).

Received 5 December 2011; accepted 18 January 2012; published online 26 February 2012; doi:10.1038/nn.3055

Th-GAL4/UAS-shi^{ts} flies were trained with one cycle of conditioning at the permissive temperature and were then shifted to the restrictive temperature during memory consolidation and retrieval (blockade was maintained during the test to avoid a potential rebound of dopamine release). This resulted in an increased memory score when flies were tested 3 h after training (**Fig. 1a**), whereas *Th-GAL4/UAS-shi^{ts}* flies showed no memory enhancement at the permissive temperature (**Supplementary Fig. 1a**) and normal olfaction at the restrictive temperature (**Supplementary Fig. 1b**). This extra memory was found to be resistant to cold-shock anesthesia (**Fig. 1b**), a hallmark of ARM[4,25]. Blocking dopaminergic neurons after five massed cycles of conditioning, which generates ARM[3] persisting for more than 1 d, yielded an increased 24-h memory performance (**Fig. 1c**) that did not occur in flies that were kept at the permissive temperature (**Supplementary Fig. 1c**). This memory enhancement was a result of blockade during the consolidation phase (**Fig. 1d**) and not during memory retrieval (**Supplementary Fig. 1d**). Taken together, these data suggest that, in wild-type flies, dopaminergic neurons' activity after conditioning controls memory consolidation by inhibiting ARM formation.

To test this hypothesis, we assessed the effect in *Th-GAL4/+; +/UAS-TrpA1* flies of a brief overactivation of dopaminergic neurons immediately after conditioning. We observed that 3-h memory was strongly decreased (**Fig. 1e**), leaving only labile memory (**Fig. 1f**), whereas *Th-GAL4/+; +/UAS-TrpA1* flies that were kept at the permissive temperature after training displayed normal memory scores (**Supplementary Fig. 1e**). Overall, these findings indicate that ARM consolidation is regulated by dopaminergic neurons after training.

Three pairs of PPL1 neurons control ARM levels

Specific behavioral functions have already been attributed to restricted subsets of *Drosophila* dopaminergic neurons[17,23]. We thus investigated whether ARM regulation could be ascribed to specific dopaminergic neurons. The expression pattern of the *NP0047-GAL4* line includes only three pairs of the mushroom body–innervating dopaminergic neurons in the PPL1 cluster, namely MB-V1 (V1) neurons, MB-MV1 (MV1) neurons and a single pair of MB-MP1 (MP1) neurons[21] (**Fig. 2a–c** and **Supplementary Movies 1** and **2**). Expression in those three pairs of dopaminergic neurons is silenced by *Th* promoter–driven GAL80 (*Th-GAL80*)[17] (**Fig. 2d,e** and **Supplementary Movies 3** and **4**). Notably, blocking *NP0047-GAL4* neurons output during the consolidation phase after massed training led to a strong increase in 24-h memory, recapitulating the effect observed with *Th-GAL4* (**Fig. 2f**). This increase was abolished by *Th-GAL80* and is therefore attributable to the V1, MV1 and MP1 dopaminergic neurons (**Fig. 2f**). *NP0047-GAL4/UAS-shi^{ts}* flies showed no memory enhancement at the permissive temperature (**Supplementary Fig. 2a**).

Transient activation of *NP0047-GAL4* neurons after one cycle of conditioning caused a memory drop that recapitulated the effect that was observed with *Th-GAL4* and was rescued by *Th-GAL80* (**Fig. 2g**). This memory drop corresponded to a specific ARM disruption (**Supplementary Fig. 2b**). *NP0047-GAL4/+; +/UAS-TrpA1* flies maintained at the permissive temperature after training showed normal memory performance (**Supplementary Fig. 2c**). Taken together, our data suggest that the activity of three specific pairs of dopaminergic neurons, namely V1, MV1 and MP1 neurons, or a subset of these neurons, tunes ARM consolidation.

MV1 and MP1 neurons display slow calcium oscillations

To functionally characterize these three dopaminergic neurons, we then made *in vivo* recordings of their activity using the fluorescent calcium reporter *GCaMP3* (ref. 26). First, we recorded naive unstimulated flies. We observed that MP1 and MV1 neurons powered large spontaneous calcium variations in their mushroom body innervations compared with control neuropils (**Fig. 3a,b**). This is not a general property of dopaminergic neurons, as projections from V1 neurons on mushroom body vertical lobes showed only noisy fluctuations, the amplitude of which did not differ from those of control neuropils (**Fig. 3a,b**). All three types of neurons had contralateral projections on symmetrical areas[19] (**Fig. 2a**). Thus, signals collected from processes targeting left and right mushroom bodies were highly synchronized in MP1 and in MV1 neurons (**Fig. 3a**). Despite having similar contralateral projections, V1 neurons showed signals with little bilateral correlation (**Fig. 3a**), which further suggests that the fluctuations observed in V1 were noise and that V1 had no spontaneous activity that was detectable at this level of sensitivity.

MP1 and MV1 neurons send out processes in close vicinity to the junction area of mushroom body lobes. When the orientation and the quality of the preparation allowed us to clearly distinguish them, we checked that both MV1 and MP1 neurons shared

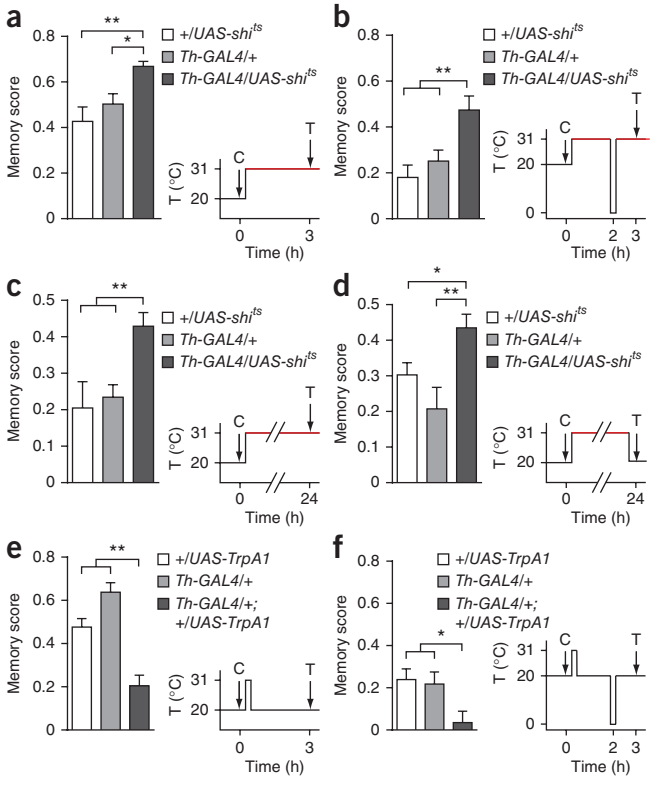

Figure 1 *Th-GAL4* neurons regulate ARM consolidation. Time courses of temperature changes are shown alongside each graph of memory performance. C, conditioning; T, test. (**a**,**b**) Blocking the output of *Th-GAL4* neurons after a single cycle of training (1x) enhanced 3-h memory ($F_{2,41} = 7.203$, $P = 0.002$, $n \geq 14$, **a**). This extra memory was resistant to a 2-min cold-shock performed 2 h after training, and thus corresponded to ARM ($F_{2,42} = 7.768$, $P = 0.0013$, $n \geq 14$, **b**). (**c**,**d**) 24-h memory after massed training was also increased ($F_{2,51} = 5.746$, $P = 0.0056$, $n \geq 18$, **c**), even when neurons were blocked during the consolidation phase only ($F_{2,42} = 6.327$, $P = 0.0040$, $n \geq 14$, **d**). (**e**,**f**) Conversely, activation of *Th-GAL4* neurons immediately after single-cycle training impaired memory ($F_{2,39} = 24.49$, $P < 0.0001$, $n \geq 14$, **e**), specifically ARM ($F_{2,39} = 4.332$, $P = 0.02$, $n \geq 14$, **f**). Data are presented as mean ± s.e.m. $^*P < 0.05$, $^{**}P < 0.01$, $^{***}P < 0.001$.

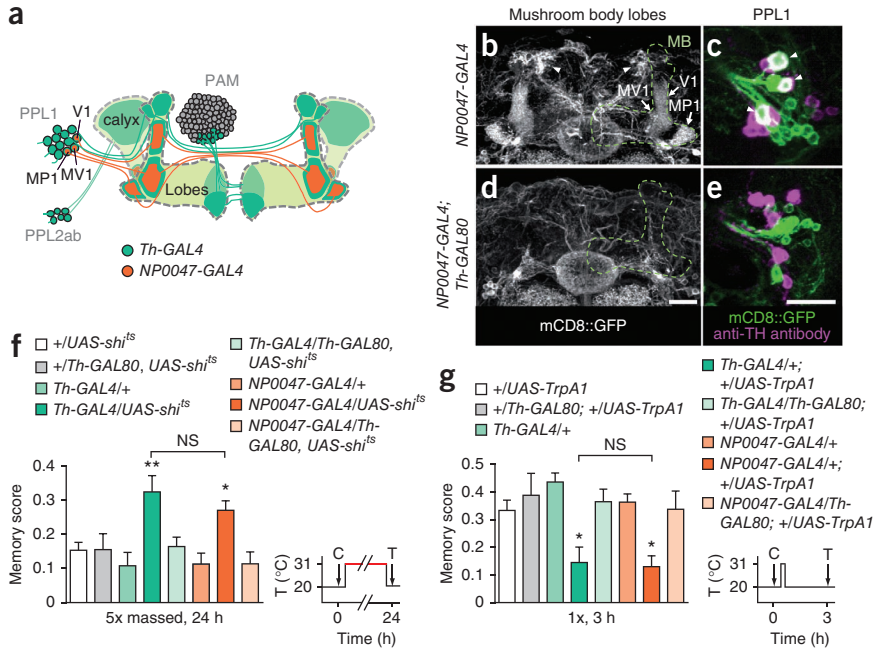

Figure 2 Three pairs of dopaminergic neurons recapitulate the ARM-regulating properties of *Th-GAL4* neurons. (**a**) Schematic drawing of mushroom body–connected dopaminergic processes. *Th-GAL4* (green) labels all cells in the PPL1 and PPL2ab clusters and 11–12 cells in the PAM cluster. *NP0047-GAL4* (orange) labels three cells in the PPL1 cluster. (**b**–**e**) The expression pattern of *NP0047-GAL4* in brain regions including the mushroom bodies (MB, frontal view, dorsal up, **b**) highlighted mushroom body projections from V1, MV1 and MP1 neurons (arrows, **b**), three tyrosine hydrdoxylase–immunoreactive cells in PPL1 cluster (arrowheads, **c**). Bright symmetrical dorsal projections are additional MP1 processes (arrowheads, **b**). *Th-GAL80* abolished expression in these three dopaminergic neurons (**d**,**e**). Scale bars represent 20 µm. See **Supplementary Movies 1–4** for expression patterns in the entire brain. (**f**,**g**) Blockade (**f**) or activation (**g**) of *NP0047-GAL4* neurons recapitulated enhancement ($F_{4,64} = 3.61$, $P = 0.01$, $n \geq 13$, **f**) and impairment ($F_{4,35} = 4.60$, $P = 0.004$, $n \geq 6$, **g**) of memory performance, respectively, obtained with *Th-GAL4* ($F_{4,53} = 4.464$, $P = 0.003$, $n \geq 9$, **f**; $F_{4,31} = 5.066$, $P = 0.0029$, $n \geq 6$, **g**). Both effects were suppressed by *Th-GAL80*. Data are presented as mean ± s.e.m. $^*P < 0.05$, $^{**}P < 0.01$; NS indicates not significant, $P \geq 0.05$.

the ability to sustain spontaneous calcium activity. Simultaneous dual-plane recordings revealed synchrony between the two types of neurons (**Fig. 3c**). As no feature proved distinguishable between signals from MV1 and MP1 neurons (**Supplementary Fig. 3**), and as most *in vivo* recordings allowed only partial discrimination between projections from each of the two neurons, we hereafter report our data as MV1 and MP1 imaging.

In naive flies, MV1 and MP1 neurons sometimes produced nonperiodic signals, which were characterized by a monotonically decreasing power spectrum with prominent low-frequency content (**Fig. 3d**). However, we found that spontaneous calcium variations in MV1 and MP1 neurons could sometimes be shaped into rhythmic oscillatory patterns, as evidenced by a peak in the power spectra of the signals of individual flies (**Fig. 3e** and **Supplementary Movie 5**).

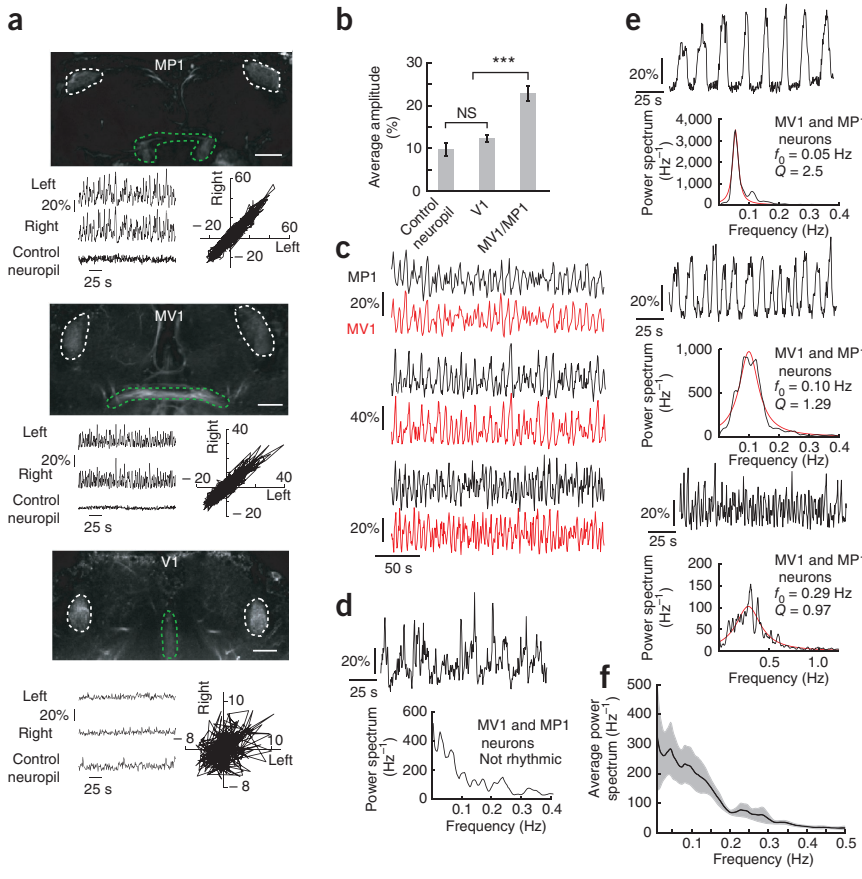

Figure 3 Spontaneous sustained activity in MV1 and MP1 neurons of naive flies. (**a**) Transverse sections of brains showing GCaMP3 fluorescence driven by *NP0047* at three different depths showing mushroom body projections of MP1 (top), MV1 (middle) and V1 (bottom) neurons (white regions of interest) and control neuropils (green). Scale bars represent 20 µm. Time courses of signals are shown below, along with correlation plots between hemispheres. (**b**) Amplitude of spontaneous activity in dopaminergic neurons and control structures ($n = 12$ flies). (**c**) Three examples of simultaneous recordings of MV1 (red) and MP1 (black) neurons showing marked synchrony. (**d**,**e**) Four illustrative examples of spontaneous activity in MV1 and MP1 neurons, including one example with no defined frequency (**d**) and three occurrences of rhythmic oscillatory signals (**e**). Power spectra are shown below each trace (black line), along with the best-fitting Lorentz curve for the rhythmic signals (red line) (see Online Methods for calculation of f_0 and Q). (**f**) Average power spectrum across all imaged flies ($n = 13$). Average data are presented as mean ± s.e.m. $^{***}P < 0.001$; NS indicates not significant, $P \geq 0.05$.

Among such oscillatory signals, frequencies were broadly distributed, ranging over one order of magnitude, from 0.03 to 0.3 Hz. Because of this wide variety of behavior, and although a majority of naive animals displayed sparse (4 of 13 flies) or robustly persistent (6 of 13) oscillatory phases, no peaked feature emerged from the power spectrum averaged across all naive animals, which decreased monotonically from 0 to 0.5 Hz (**Fig. 3f**).

MV1 and MP1 oscillations correlate with ARM processing

We next investigated whether sustained activity of dopaminergic neurons was physiologically associated with ARM processing. After one cycle of associative training, a large majority of flies displayed rhythmic oscillations in MV1 and MP1 neurons (**Fig. 4a**). Indeed, a significantly higher number of flies that underwent single-cycle training displayed persistent oscillations compared with flies that underwent an unpaired conditioning (9 of 11 flies versus 4 of 11, $P = 0.036$, two-tailed Fisher's exact test). Consistently, significant differences in the ensemble power spectra after both protocols were a result of the low-frequency content (**Fig. 4b**), which, in naive flies, mostly came from nonrhythmic cases (**Fig. 3d**). Single-cycle–trained flies thus showed a peaked power spectrum (**Fig. 4b**) that was still quite broad because of frequency dispersion (central frequency $f_0 = 0.13$ Hz, quality factor $Q = 0.72$). As a consequence, the frequency and the quality factor of MV1 and MP1 activity were globally higher in single-cycle–trained flies than in unpaired-conditioned flies (**Fig. 4c**,**d**) during the assayed period, which extended over more than 1 h after conditioning. Noticeably, the amplitudes of MV1 and MP1 activity followed identical time courses in single-cycle–trained flies and unpaired-conditioned flies (**Fig. 4e**), which suggests that single-cycle training induces essentially qualitative changes through an increased tendency of MV1 and MP1 neurons to oscillate. As in naive flies, no above-noise activity could be measured in V1 neurons after single-cycle training (**Supplementary Fig. 4**).

As shown above (**Fig. 1b**), ARM levels were increased by blocking dopaminergic neurons activity during the time period in which preferential oscillatory behavior of MV1 and MP1 neurons occurs. We therefore hypothesized that MV1 and MP1 oscillations mediate ARM inhibition. Given that ARM is decreased by a short overactivation of *NP0047-GAL4* neurons in heat-stimulated *NP0047-GAL4/+; +/UAS-TrpA1* flies (**Fig. 2g**), we asked whether MV1 and MP1 oscillations were enhanced in these flies. Unfortunately, *UAS-GCaMP3, UAS-TrpA1/+; NP0047-GAL4/+* flies had a 3-h memory defect at permissive temperature that was absent in *UAS-GCaMP3/+; NP0047-GAL4/+* flies (**Supplementary Fig. 5a**) and in *UAS-TrpA1/+; NP0047-GAL4/+* flies (**Supplementary Fig. 1e**). In addition, simultaneous expression of *GCaMP3* and *TrpA1* in *NP0047-GAL4* neurons abolished the sustained activity of MV1 and MP1 neurons in naive flies ($n = 10$; **Supplementary Fig. 5b**). However, a brief stimulation of MV1 and MP1 neurons by *TrpA1* activation (see Online Methods) gave rise to a period of sustained activity that persisted for at least 45 min and could be oscillatory (**Supplementary Fig. 5b**,**c**). This did not occur in heat-stimulated *UAS-GCaMP3; NP0047-GAL4/+* control flies that did not carry *UAS-TrpA1* (**Supplementary Fig. 5d**). These results suggest that MV1 and MP1 oscillations inhibit ARM, even though they should be considered cautiously because MV1 and MP1 neurons' physiology is altered in *UAS-GCaMP3, UAS-TrpA1/+; NP0047-GAL4/+* flies.

If MV1 and MP1 oscillations are detrimental to ARM consolidation, we expect that massed training that promotes high levels of day-lasting ARM[3] will negatively affect those oscillations. In massed-trained flies (**Fig. 4f**), MV1 and MP1 neurons were seldom oscillatory (4 of 11 flies) and showed otherwise irregular non-oscillating activity (4 of 11 flies) or were completely quiet (3 of 11 flies). Thus, the proportion of massed-trained flies showing oscillatory activity in MV1 and MP1 neurons was decreased compared with single-cycle–trained flies (4 of 11 massed-trained flies versus 9 of 11 single-cycle–trained flies, $P = 0.036$, two-tailed Fisher's exact test), which resulted in a

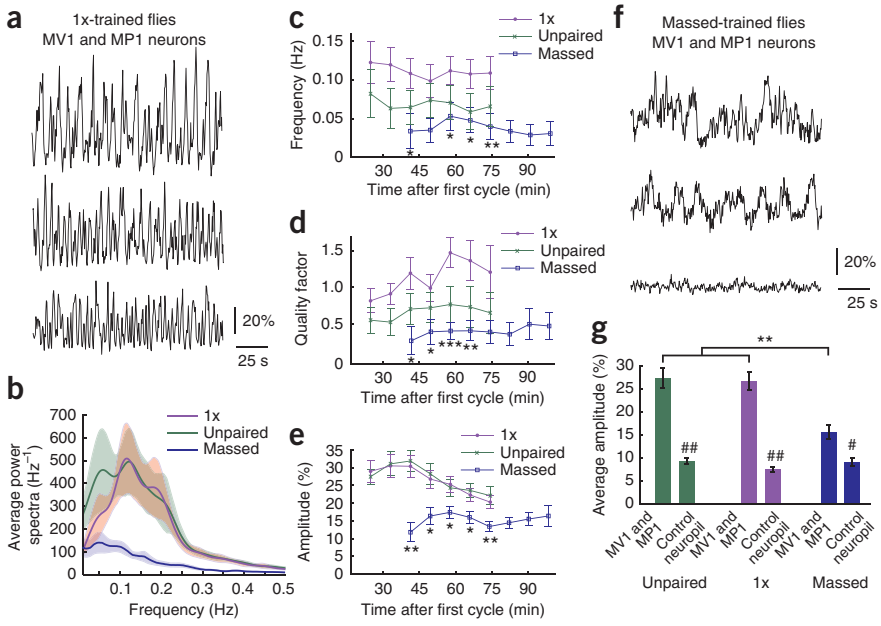

Figure 4 Oscillations in MV1 and MP1 neurons are correlated with ARM regulation. (**a**) Illustrative examples of recordings from MV1 and MP1 neurons 30–45 min after one cycle of associative conditioning. (**b**) Average power spectra across all tested animals obtained after single-cycle, unpaired and massed training. Significant differences between single-cycle and unpaired spectra on the whole frequency range (comparison from 0 to 0.3 Hz: $F_{1,3167} = 14.25$, $P = 0.0002$, two-way ANOVA) were actually a result of the low frequency range (no significant difference from 0.1 to 0.3 Hz: $F_{1,2220} = 0.05$, $P = 0.82$, two-way ANOVA). (**c**–**e**) Time courses of the frequency (**c**), quality factor (**d**) and amplitude (**e**) in MV1 and MP1 neurons after single-cycle, unpaired and massed training. Asterisks denote significant differences between massed and single-cycle training at a given time point. There were no significant differences between single-cycle training and unpaired curves at a given time point, but the global time courses were significantly different between the two conditions regarding frequency ($F_{1,153} = 11.14$, $P = 0.0011$, two-way ANOVA) and quality factor ($F_{1,153} = 12.21$, $P = 0.0006$, two-way ANOVA), but not amplitude ($F_{1,153} = 0.45$, $P = 0.50$, two-way ANOVA). (**f**) Illustrative examples of recordings from MV1 and MP1 neurons 30–45 min after massed training. (**g**) Average amplitude of signals recorded from MV1 and MP1 neurons and control structures after single-cycle, unpaired and massed training. Signals from dopaminergic neurons were lower after massed than after single-cycle or unpaired protocols ($F_{2,32} = 11.93$, $P = 0.0002$). # symbols denote a significant difference between MV1 and MP1 and the control for a given protocol ($^{\#}P < 0.05$, $^{\#\#}P < 0.01$). $n = 11$ flies for each condition. Average data are presented as mean ± s.e.m. $^{*}P < 0.05$, $^{**}P < 0.01$, $^{***}P < 0.001$.

monotonically decreasing power spectrum for massed-trained flies (**Fig. 4b**) and a marked drop of the average frequency and quality factor compared with single-cycle–trained flies (**Fig. 4d**,**e**). Moreover, massed training also induced a decrease of the amplitude of MV1 and MP1 activity (**Fig. 4c**). This amplitude, however, remained above those of control neuropils (**Fig. 4g**), consistently with the fact that full blockade of *NP0047-GAL4* dopaminergic neurons output after massed conditioning could further increase 24-h ARM (**Fig. 2f**). As for single-cycle training, no detectable activity appeared in V1 neurons after massed training (**Supplementary Fig. 4**).

Thus, although one cycle of conditioning favored oscillatory behavior of MV1 and MP1 neurons, juxtaposing four additional cycles right after the first one, which allows persistent ARM consolidation, suppressed the effect. Altogether, our data suggest that MV1 and MP1 oscillations are negatively correlated with ARM consolidation.

We next asked whether the *radish* (*rsh*) gene, which encodes a protein that is required for ARM consolidation and is expressed in the mushroom bodies[25,27], is somehow linked to the pathway controlled by MV1 and MP1 oscillations. In *rsh* mutant flies, MV1 and MP1 oscillations were normal in terms of frequency distribution, average spectrum (**Supplementary Fig. 6a**) and amplitude (**Supplementary Fig. 6b**). Consistent with this, blocking dopaminergic neurons of either *rsh*/+ females or *rsh*/*Y* males after single-cycle training still resulted in increased memory performance (**Supplementary Fig. 6c**). These results suggest that *rsh* and MV1 and MP1 neurons affect ARM consolidation through independent pathways.

ARM is absent when LTM is formed

As previously mentioned, two forms of consolidated memories exist in *Drosophila*, ARM and protein synthesis–dependent LTM. It is well established that ARM forms after massed training, whereas LTM only forms after multiple cycles of conditioning spaced by an ITI of typically 15 min (ref. 3) We previously proposed that ARM and LTM are exclusive memory phases, meaning that ARM is inhibited after spaced training[4]. This last point is, however, debated, as it is often stated that ARM is normally present after spaced training[3,6]. Here we provide three additional lines of evidence to further demonstrate that ARM is inhibited when LTM is formed.

First, arguments against the exclusive memories model are frequently based on the fact that most flies with abnormal LTM show, after spaced conditioning, a significant residual memory that could correspond to ARM[3,6]. Using cycloheximide (CXM), an inhibitor of protein synthesis, to probe the formation of LTM, we analyzed the quality of residual memory of two loss-of-function mutants, *crammer* (*cer*)[28] and *tequila* (*teq*)[29], that specifically affect LTM. We first checked that both *cer* and *teq* fed with CXM had a normal memory performance after massed conditioning (**Fig. 5a**), confirming that both CXM treatment and the concerned mutations do not affect ARM. After spaced conditioning, *cer* and *teq* memory was strongly decreased by CXM treatment (**Fig. 5a**). Thus, the residual memory observed in *cer* and *teq* LTM mutants corresponds to partial LTM, and not to normal ARM, confirming that ARM is inhibited when LTM is formed[4].

Second, it was recently shown that feeding flies with DL-p-chlorophenylalanine (pCPA), an inhibitor of serotonin synthesis, specifically impairs ARM 3 h after single-cycle training as well as 24 h after massed training[30]. We confirmed that pCPA treatment impaired the memory of wild-type flies after massed training (**Fig. 5b**). Notably, the 24-h memory of wild-type flies fed with pCPA was normal after spaced training (**Fig. 5b**), strongly suggesting that ARM is absent after spaced training.

Third, to inhibit ARM, we briefly activated *Th-GAL4* neurons after each conditioning cycle of the spaced and massed protocols using *TrpA1*. We performed a massed training with a short 5-min ITI, a duration that is insufficient to properly achieve LTM formation[31], but leaves enough time to briefly overactivate *Th-GAL4* neurons between each cycle. As expected from the single-cycle training experiment (**Fig. 1e**,**f**), the 24-h memory of *Th-GAL/+; +/UAS-TrpA1* flies was strongly decreased after massed training (**Fig. 5c**). We performed a control experiment to check that *Th-GAL4/+; +/UAS-TrpA1* flies learned normally after a single cycle of training preceded by thermal activation (**Supplementary Fig. 7a**), ensuring that the measured defect after massed conditioning was actually a result of ARM impairment after conditioning and not of a putative interference of the procedure with learning itself. Activation of *Th-GAL4* neurons right after each cycle of a spaced protocol did not alter 24 h memory (**Fig. 5d**). Overall, these data indicate that ARM is either blocked or erased by spaced training, which therefore only induces LTM formation.

Spaced training promotes MV1 and MP1 neurons oscillations

We next asked whether ARM-inhibiting MV1 and MP1 neurons are involved in the complete ARM blockade caused by spaced training. Indeed, a significantly higher number of spaced-trained flies showed long-lasting oscillations in MV1 and MP1 neurons than in flies that underwent a control spaced unpaired conditioning (10 of 11 space-trained flies versus 3 of 11 unpaired flies, $P = 0.004$, two-tailed Fisher's exact test). Spaced-trained flies consistently displayed persistent oscillations in a restricted frequency range around 0.1 Hz (**Fig. 6a**), which resulted in a well-defined peak in the average spectrum ($f_0 = 0.11$ Hz, $Q = 1.11$; **Fig. 6b**). In comparison, unpaired flies produced a non-oscillatory monotonous ensemble spectrum (**Fig. 6b**).

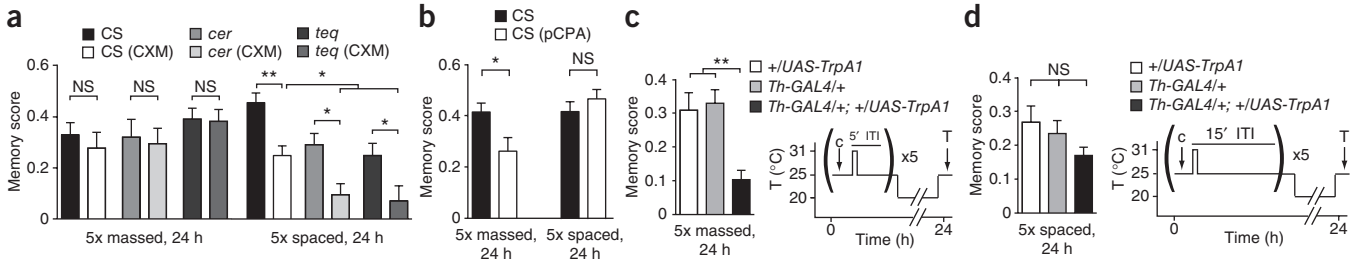

Figure 5 ARM is absent after spaced conditioning. (**a**) Effect of CXM on specific LTM mutants *cer* and *teq*. Memory scores in different groups were similar 24 h after massed conditioning ($F_{5,44} = 0.657$, $P = 0.66$, $n = 8$). Conversely, there were significant differences between groups 24 h after spaced conditioning ($F_{5,119} = 10.22$, $P < 0.0001$, $n \geq 18$). CS, Canton Special. (**b**) ARM-affecting pCPA treatment resulted in a defect of 24-h memory after massed training ($P = 0.024$, $n = 12$), but not after spaced training ($P = 0.36$, $n = 15$). (**c**,**d**) 24-h memory was significantly affected after brief overactivation of *Th-GAL4* neurons after each cycle of a massed training ($F_{2,35} = 9.03$, $P = 0.0006$, $n = 12$, **c**), but not after spaced training ($F_{2,38} = 1.71$, $P = 0.19$, $n = 12$, **d**). Data are presented as mean ± s.e.m. $^*P < 0.05$, $^{**}P < 0.01$; NS indicates not significant, $P \geq 0.05$.

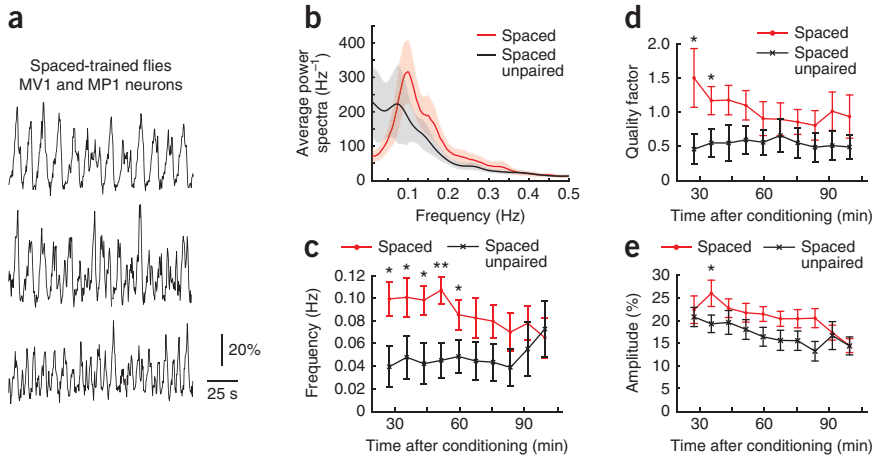

Figure 6 Spaced training consistently promotes oscillatory behavior in MV1 and MP1 neurons. (**a**) Illustrative recordings from MV1 and MP1 neurons obtained 30–60 min after spaced conditioning. (**b**) Average power spectrum across all tested flies obtained after spaced conditioning was significantly different from that produced by a spaced unpaired protocol (comparison from 0 to 0.3 Hz: $F_{1,3167} = 19.3$, $P = 1.2 \times 10^{-5}$, two-way ANOVA, $n = 11$ flies for each condition). (**c**–**e**) Time courses of the frequency (**c**), quality factor (**d**) and amplitude (**e**) of activity in MV1 and MP1 neurons after spaced training and spaced unpaired protocol. Global comparison of time courses proved significantly different for all three parameters (frequency, $F_{1,175} = 35.23$, $P < 0.0001$; quality factor, $F_{1,175} = 16.94$, $P = 0.0001$; amplitude, $F_{1,175} = 17.91$, $P < 0.0001$; two-way ANOVA). Average data are presented as mean ± s.e.m. $^*P < 0.05$, $^{**}P < 0.01$.

Comparison of the time courses of the frequency and quality factor up to 1.5 h after conditioning revealed that activity patterns of MV1 and MP1 neurons in spaced-trained flies were faster (**Fig. 6c**) and more regularly cadenced (**Fig. 6d**) than in unpaired flies. During the first hour after training, the magnitude of differences, and thus the discrimination between trained and unpaired flies, were even more strongly marked than during the same time period after only one cycle of training (**Figs. 4c**,**d** and **6c**,**d**). In addition, spaced-training induced a quantitative effect on the amplitude of MV1 and MP1 activity, which was higher in trained flies than in unpaired flies (**Fig. 6e**). Similar to other protocols, spaced training did not affect V1 neurons activity after conditioning (**Supplementary Fig. 4**). Thus, the ARM-inhibiting spaced protocol strongly drives MV1 and MP1 neurons into an ARM-opposing oscillatory behavior.

ARM-regulating neurons gate LTM formation

We then sought to understand the physiological rationale of ARM inhibition by MV1 and MP1 oscillating neurons after spaced training. We blocked *Th-GAL4* neurons from the end of a spaced protocol throughout the consolidation phase. This treatment did not affect LTM (**Fig. 7a**). Given that spaced training lasts 1.5 h and that the training-evoked promotion of MV1 and MP1 oscillations started to occur after the first cycle of training (**Fig. 4**), we reasoned that the major part of physiologically relevant events could occur during the spaced training itself rather than during the consolidation phase. Thus, after checking that *Th-GAL4/UAS-shi^{ts}* flies could appropriately form LTM when spaced trained at the permissive temperature (**Fig. 7b**), and that blocking *Th-GAL4* neurons for 8 min before single-cycle training did not impair learning (**Supplementary Fig. 7b**), we designed a protocol to block neuronal activity during the first 8 min of each 15-min ITI of a spaced training (**Fig. 7c**). Despite multiple temperature shifts during the spaced training (**Fig. 7c**), control flies formed LTM (**Fig. 7d**), but blocking *Th-GAL4* neurons during ITIs and early consolidation prevented LTM formation, leaving only CXM-insensitive ARM (**Fig. 7d**).

To determine whether this effect was a result of ARM-controlling neurons, we conducted the same series of experiments with *NP0047-GAL4/UAS-shi^{ts}* flies. We first determined that LTM formation was normal when these flies were trained at the permissive temperature (**Fig. 7b**) and that learning during single-cycle

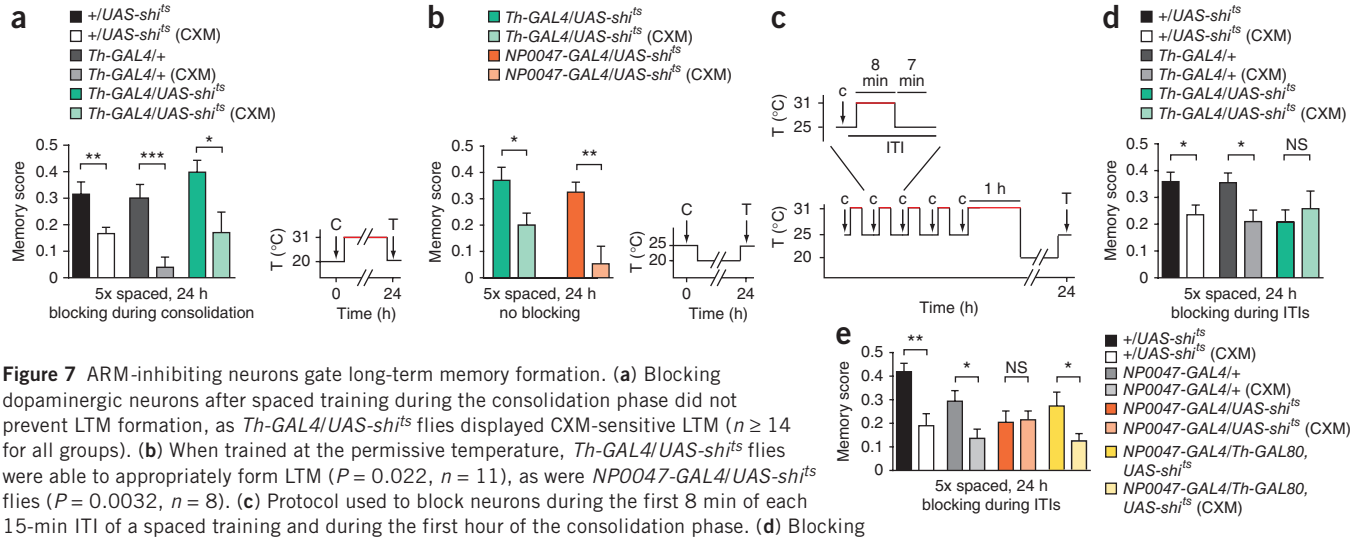

Figure 7 ARM-inhibiting neurons gate long-term memory formation. (**a**) Blocking dopaminergic neurons after spaced training during the consolidation phase did not prevent LTM formation, as *Th-GAL4/UAS-shi^{ts}* flies displayed CXM-sensitive LTM ($n \geq 14$ for all groups). (**b**) When trained at the permissive temperature, *Th-GAL4/UAS-shi^{ts}* flies were able to appropriately form LTM ($P = 0.022$, $n = 11$), as were *NP0047-GAL4/UAS-shi^{ts}* flies ($P = 0.0032$, $n = 8$). (**c**) Protocol used to block neurons during the first 8 min of each 15-min ITI of a spaced training and during the first hour of the consolidation phase. (**d**) Blocking *Th-Gal4* neurons according to the protocol shown in **c** precluded LTM formation (+/*UAS-shi^{ts}*, $P = 0.021$; *Th-GAL4/+*, $P = 0.016$; *Th-GAL4/UAS-shi^{ts}*, $P = 0.54$; $n \geq 12$ for all groups). (**e**) As with *Th-Gal4* neurons, LTM formation was abolished when *NP0047-GAL4* neurons were blocked during the ITI and the first hour after conditioning. This was because of the three pairs of *NP0047-GAL4* dopaminergic neurons, as the ability to form LTM was recovered in combination with *Th-GAL80* (+/*UAS-shi^{ts}*, $P = 0.0014$; *NP0047-GAL4/+*, $P = 0.014$; *NP0047-GAL4/UAS-shi^{ts}*, $P = 0.86$; *NP0047-GAL4/Th-GAL80, UAS-shi^{ts}*, $P = 0.038$; $n \geq 11$ for all groups). Data are presented as mean ± s.e.m. $^*P < 0.05$, $^{**}P < 0.01$, $^{***}P < 0.001$; NS indicates not significant, $P \geq 0.05$.

training was normal after blockade of *NP0047-GAL4* neurons (**Supplementary Fig. 7c**). As with *Th-GAL4* neurons, blocking ARM-opposing *NP0047-GAL4* neurons during the ITIs of a spaced training abolished CXM sensitivity of 24-h memory, whereas LTM was intact in genotypic controls (**Fig. 7e**). This LTM loss was actually attributable to the three pairs of ARM-regulating dopaminergic neurons, as the presence of *Th-GAL80* rescued LTM formation (**Fig. 7e**). In conclusion, those data indicate that in the absence of ARM inhibition, LTM cannot form and that *NP0047-GAL4* dopaminergic neurons gate LTM formation during the ITI of spaced conditioning.

DISCUSSION

We addressed the role of dopaminergic neurons in aversive memory consolidation and found that dopaminergic neurons are specifically involved in the regulation of the anesthesia-resistant component of olfactory memory. More specifically, we found that as few as three pairs of mushroom body–projecting dopaminergic neurons from the PPL1 cluster, V1, MV1 and MP1, inhibit ARM formation after aversive olfactory learning of normal flies. *In vivo* calcium imaging experiments in unstimulated flies revealed that MV1 and MP1, but not V1, neurons displayed a highly synchronized sustained activity that was sometimes shaped into rhythmic oscillations. In trained flies, the strength of MV1 and MP1 oscillations was tightly correlated with ARM processing.

In terms of neural circuitry, the inputs of MV1 and MP1 neurons are unknown, raising the question of whether they are isolated self-oscillators or are part of a larger oscillating circuit. The fact that MV1 and MP1 oscillations are in phase, both in the same hemisphere and across hemispheres, favors the second hypothesis.

The molecular pathways by which dopaminergic neurons activity could regulate ARM remain elusive. We found that ARM regulation by dopaminergic neurons do not rely on the products of the *rsh* gene. Activation of protein kinase A has been shown to inhibit ARM in the mushroom body[32]. Dopamine release from the MV1 and MP1 neurons could trigger cAMP production and increased protein kinase A activity in the mushroom body[33,34], thereby inhibiting ARM.

In the framework of memory phases, we previously proposed that ARM and LTM are exclusive consolidated memories[4], a model that has been debated[6]. Our results support the idea that ARM is inhibited after spaced conditioning, when LTM is formed. Why is ARM inhibited when LTM is formed? When the three pairs of ARM-inhibiting dopaminergic neurons were blocked between the multiple cycles of a spaced training, LTM formation was voided. Consistent with these results, *in vivo* calcium imaging showed that a single cycle and, more strongly, a spaced training fostered MV1 and MP1 oscillatory activity, whereas a massed training inhibited MV1 and MP1 oscillations.

These results consistently point to a plausible model of consolidated memory phases in *Drosophila*, in which oscillations of dopaminergic neurons gate the formation of LTM by tuning the ARM pathway (**Supplementary Fig. 8**). In this model, two parallel mutually inhibiting pathways can lead to the formation of day-lasting ARM or LTM. After a single cycle or massed conditioning, the ARM pathway is activated and prevents LTM formation. During the rest intervals of the spaced conditioning MV1 and MP1 oscillations are enhanced and the ARM pathway is therefore inhibited and LTM can form in relevant mushroom body neurons.

Although we have identified ARM-regulating neurons, the mechanisms by which ARM, or physiological events leading to it, prevents LTM formation remain to be elucidated. The spacing effect, that is, the fact that stronger memory is formed when multiple trainings are spaced over time compared with the same number of trainings without spacing, is widely established in the animal kingdom[35]. Notably, the gating of LTM formation occurred during the ITIs of spaced training in our experiments. Recently, it has been shown that the duration of the ITI required to form LTM in *Drosophila* is regulated by the *corkscrew* gene through waves of Ras/mitogen-activated protein kinase activity[35]. It will be interesting to investigate a putative interaction between mitogen-activated protein kinase waves and MV1 and MP1 oscillatory activity, and to determine whether stimulating oscillations during the ITI facilitates LTM formation, for example, with shorter ITIs or with fewer conditioning cycles.

We identified dopaminergic neurons whose activity inhibits ARM and therefore, as in mammals, positively affects LTM formation[10]. That regulation of memory consolidation seems to involve precisely cadenced oscillations in MV1 and MP1 neurons is of particular conceptual interest. Indeed, it was recently suggested that a subset of hypothalamic dopaminergic neurons in rats, robustly oscillating at 0.05 Hz, may be responsible for lactation inhibition[36]. Thus, inhibition through rhythmic oscillations appears to be a widespread functional feature of dopaminergic networks. In addition, a slow oscillatory firing mode, in the 0.5–1.5-Hz frequency range, has been identified in the dopaminergic neurons in the ventral tegmental area of rats[37]. This oscillatory firing pattern would underlie subsecond synchronization between ventral tegmental area and prefrontal cortex[38], an area of major importance in learning and memory[39]. Thus, and although such an assumption remains quite speculative, LTM regulation by dopaminergic neurons in mammals might involve mechanisms similar to those described here in *Drosophila*.

METHODS

Methods and any associated references are available in the online version of the paper at http://www.nature.com/natureneuroscience/.

Note: Supplementary information is available on the Nature Neuroscience website.

ACKNOWLEDGMENTS

We thank A. Pascual (Instituto de Biomedicina de Sevilla) and members of the Genes and Dynamics of Memory Systems group for critical reading of the manuscript. This work was supported by grants from the Agence Nationale pour la Recherche (T.P.), the Fondation pour la Recherche Médicale (T.P.), the Fondation Bettencourt-Schueller (T.P.), the Emmy-Noether Program from Deutsche Forschungsgemeinschaft (H.T.), the Bernstein focus Learning from Bundesministerium für Bildung und Forschung (H.T.) and the Max-Planck-Gesellschaft (H.T.). P.-Y.P. was supported by a grant from Région Ile-de-France, G.I. and S.T. by the Fondation pour la Recherche Médicale, and Y.A. by Deutscher Akademischer Austausch Dienst.

AUTHOR CONTRIBUTIONS

S.B., G.I. and T.P. were involved in the original design of the study. Behavioral experiments were performed by G.I. (**Figs. 1**, **5a** and **7a**, and **Supplementary Fig. 1**), S.T. (**Figs. 2**, **5c**,**d** and **7b**,**d**,**e**, and **Supplementary Figs. 2** and **7**), P.-Y.P. (**Fig. 5b** and **Supplementary Fig. 5a**) and G.B.-G. (**Supplementary Fig. 6c**). P.-Y.P. carried out all of the calcium imaging experiments and data analyses, except for the *rsh* experiment that was perfomed by G.B.-G. (**Supplementary Fig. 6a**,**b**). Y.A., I.S. and H.T. performed immunohistochemistry and analyzed the results. S.B. provided some fly stocks. P.V. provided financial support. P.-Y.P. and T.P. wrote the manuscript. T.P. designed the study and supervised the work. All of the authors discussed the results and commented on the manuscript.

COMPETING FINANCIAL INTERESTS

The authors declare no competing financial interests.

Published online at http://www.nature.com/natureneuroscience/.
Reprints and permissions information is available online at http://www.nature.com/reprints/index.html.

1. Neumann, N. *et al.* The mind of the mnemonists: an MEG and neuropsychological study of autistic memory savants. *Behav. Brain Res.* **215**, 114–121 (2010).
2. Treffert, D.A. The savant syndrome: an extraordinary condition. A synopsis: past, present, future. *Phil. Trans. R. Soc. Lond. B* **364**, 1351–1357 (2009).
3. Tully, T., Preat, T., Boynton, S.C. & Del Vecchio, M. Genetic dissection of consolidated memory in *Drosophila*. *Cell* **79**, 35–47 (1994).

4. Isabel, G., Pascual, A. & Preat, T. Exclusive consolidated memory phases in *Drosophila*. *Science* **304**, 1024–1027 (2004).
5. Mery, F. & Kawecki, T.J. A cost of long-term memory in *Drosophila*. *Science* **308**, 1148 (2005).
6. Margulies, C., Tully, T. & Dubnau, J. Deconstructing memory in *Drosophila*. *Curr. Biol.* **15**, R700–R713 (2005).
7. Wise, R.A. Dopamine, learning and motivation. *Nat. Rev. Neurosci.* **5**, 483–494 (2004).
8. O'Carroll, C.M., Martin, S.J., Sandin, J., Frenguelli, B. & Morris, R.G.M. Dopaminergic modulation of the persistence of one-trial hippocampus-dependent memory. *Learn. Mem.* **13**, 760–769 (2006).
9. Bethus, I., Tse, D. & Morris, R.G.M. Dopamine and memory: modulation of the persistence of memory for novel hippocampal NMDA receptor-dependent paired associates. *J. Neurosci.* **30**, 1610–1618 (2010).
10. Rossato, J.I., Bevilaqua, L.R.M., Izquierdo, I., Medina, J.H. & Cammarota, M. Dopamine controls persistence of long-term memory storage. *Science* **325**, 1017–1020 (2009).
11. Waddell, S. Dopamine reveals neural circuit mechanisms of fly memory. *Trends Neurosci.* **33**, 457–464 (2010).
12. Riemensperger, T. *et al.* Behavioral consequences of dopamine deficiency in the *Drosophila* central nervous system. *Proc. Natl. Acad. Sci. USA* **108**, 834–839 (2011).
13. Tully, T. & Quinn, W.G. Classical conditioning and retention in normal and mutant *Drosophila melanogaster*. *J. Comp. Physiol. [A]* **157**, 263–277 (1985).
14. Keene, A.C. & Waddell, S. *Drosophila* olfactory memory: single genes to complex neural circuits. *Nat. Rev. Neurosci.* **8**, 341–354 (2007).
15. Schwaerzel, M. *et al.* Dopamine and octopamine differentiate between aversive and appetitive olfactory memories in *Drosophila*. *J. Neurosci.* **23**, 10495–10502 (2003).
16. Claridge-Chang, A. *et al.* Writing memories with light-addressable reinforcement circuitry. *Cell* **139**, 405–415 (2009).
17. Aso, Y. *et al.* Specific dopaminergic neurons for the formation of labile aversive memory. *Curr. Biol.* **20**, 1445–1451 (2010).
18. Zhang, S., Yin, Y., Lu, H. & Guo, A. Increased dopaminergic signaling impairs aversive olfactory memory retention in *Drosophila*. *Biochem. Biophys. Res. Commun.* **370**, 82–86 (2008).
19. Mao, Z. & Davis, R.L. Eight different types of dopaminergic neurons innervate the *Drosophila* mushroom body neuropil: anatomical and physiological heterogeneity. *Front. Neural Circuits* **3**, 5 (2009).
20. Heisenberg, M. Mushroom body memoir: from maps to models. *Nat. Rev. Neurosci.* **4**, 266–275 (2003).
21. Tanaka, N.K., Tanimoto, H. & Ito, K. Neuronal assemblies of the *Drosophila* mushroom body. *J. Comp. Neurol.* **508**, 711–755 (2008).
22. Kitamoto, T. Conditional modification of behavior in *Drosophila* by targeted expression of a temperature-sensitive *shibire* allele in defined neurons. *J. Neurobiol.* **47**, 81–92 (2001).
23. Krashes, M.J. *et al.* A neural circuit mechanism integrating motivational state with memory expression in *Drosophila*. *Cell* **139**, 416–427 (2009).
24. Friggi-Grelin, F. *et al.* Targeted gene expression in *Drosophila* dopaminergic cells using regulatory sequences from tyrosine hydroxylase. *J. Neurobiol.* **54**, 618–627 (2003).
25. Folkers, E., Drain, P. & Quinn, W.G. Radish, a *Drosophila* mutant deficient in consolidated memory. *Proc. Natl. Acad. Sci. USA* **90**, 8123–8127 (1993).
26. Tian, L. *et al.* Imaging neural activity in worms, flies and mice with improved GCaMP calcium indicators. *Nat. Methods* **6**, 875–881 (2009).
27. Folkers, E., Waddell, S. & Quinn, W.G. The *Drosophila* radish gene encodes a protein required for anesthesia-resistant memory. *Proc. Natl. Acad. Sci. USA* **103**, 17496–17500 (2006).
28. Comas, D., Petit, F. & Preat, T. *Drosophila* long-term memory formation involves regulation of cathepsin activity. *Nature* **430**, 460–463 (2004).
29. Didelot, G. *et al.* Tequila, a neurotrypsin ortholog, regulates long-term memory formation in *Drosophila*. *Science* **313**, 851–853 (2006).
30. Lee, P.-T. *et al.* Serotonin-mushroom body circuit modulating the formation of anesthesia-resistant memory in *Drosophila*. *Proc. Natl. Acad. Sci. USA* **108**, 13794–13799 (2011).
31. Yin, J.C., Del Vecchio, M., Zhou, H. & Tully, T. CREB as a memory modulator: induced expression of a dCREB2 activator isoform enhances long-term memory in *Drosophila*. *Cell* **81**, 107–115 (1995).
32. Horiuchi, J., Yamazaki, D., Naganos, S., Aigaki, T. & Saitoe, M. Protein kinase A inhibits a consolidated form of memory in *Drosophila*. *Proc. Natl. Acad. Sci. USA* **105**, 20976–20981 (2008).
33. Gervasi, N., Tchénio, P. & Preat, T. PKA dynamics in a *Drosophila* learning center: coincidence detection by rutabaga adenylyl cyclase and spatial regulation by dunce phosphodiesterase. *Neuron* **65**, 516–529 (2010).
34. Tomchik, S.M. & Davis, R.L. Dynamics of learning-related cAMP signaling and stimulus integration in the *Drosophila* olfactory pathway. *Neuron* **64**, 510–521 (2009).
35. Pagani, M.R., Oishi, K., Gelb, B.D. & Zhong, Y. The phosphatase SHP2 regulates the spacing effect for long-term memory induction. *Cell* **139**, 186–198 (2009).
36. Lyons, D.J., Horjales-Araujo, E. & Broberger, C. Synchronized network oscillations in rat tuberoinfundibular dopamine neurons: switch to tonic discharge by thyrotropin-releasing hormone. *Neuron* **65**, 217–229 (2010).
37. Shi, W.-X. Slow oscillatory firing: a major firing pattern of dopamine neurons in the ventral tegmental area. *J. Neurophysiol.* **94**, 3516–3522 (2005).
38. Gao, M. *et al.* Functional coupling between the prefrontal cortex and dopamine neurons in the ventral tegmental area. *J. Neurosci.* **27**, 5414–5421 (2007).
39. Benchenane, K. *et al.* Coherent theta oscillations and reorganization of spike timing in the hippocampal-prefrontal network upon learning. *Neuron* **66**, 921–936 (2010).

ONLINE METHODS

Stocks. *Drosophila melanogaster*, wild-type *Canton Special* and mutant flies were reared at 18 °C with 60% humidity in a 12-h light-dark cycle and on a standard medium, except for *NP0047-GAL4* × *UAS-GCaMP3* crosses, which were raised at 25 °C for imaging experiments. *Th-GAL4*, *NP0047-GAL4*, *Th-GAL80*, *UAS-TrpA1*, *UAS-shi^{ts}* and *UAS-GCaMP3* flies were outcrossed for five generations to a *w^{1118}* strain carrying a *Canton Special* genetic background.

Behavioral experiments. Conditioning and test of memory performance and of olfactory acuity were performed as described previously[40,41]. Three types of training protocols were used in this study: single cycle, massed training (one training cycle repeated five times without intervals between each cycle) and spaced training (one training cycle repeated five times with a 15-min ITI between each cycle). In one experiment (**Fig. 5c**), a short 5-min ITI occurred during massed training to allow for brief thermal activation between each cycle. During an unpaired cycle of conditioning, flies were delivered the same amount of shocks 3 min before they were sequentially exposed to the two odorants.

When not indicated otherwise, conditioning and testing were performed at 25 °C. Time courses of the temperature shifts employed during experiments involving thermosensitive tools are shown alongside each graph of memory performance, and periods of neurotransmission blockade by *shi^{ts}* are highlighted in red. For blockade during consolidation, flies where placed at the restrictive temperature (31 °C) immediately after conditioning in pre-heated vials. When the temperature of the test was different from that of the consolidation phase, flies were transferred to the testing temperature 30 min before the test.

For experiments involving blockade during the ITIs of spaced conditioning, barrels with flies were plugged on a 31 °C non-odorized airflow for 8 min at the end of each cycle, then moved back to 25 °C air flow for the remaining 7 min of the ITI. At the end of the training protocol, trained flies were collected and transferred for 1 h at 31 °C in pre-heated vials. For overactivation experiments with *TrpA1*, flies were transferred in pre-heated vials at 31 °C for 1 min immediately after training.

Cold anesthesia was performed 2 h after training and achieved by a 2-min cold shock at 0 °C in pre-chilled tubes[4].

CXM was used to examine the formation of protein synthesis–dependent LTM[3] and pCPA was used to examine the formation of ARM[30]. The vehicle solution for drug feeding was mineral water (Evian) supplemented with 5% sucrose. The protocol for CXM treatment was derived from that described in ref. 42. After 1 d on fresh medium, flies were transferred into 15-ml Falcon tubes containing a Whatman filter paper (1 × 2.5 cm^2) soaked with 125 µl of 35 mM CXM solution (94% purity, Sigma, C7698) in vehicle or with vehicle alone (control) for 15–18 h at 25 °C. For pCPA treatment, 1-d-old flies were transferred for 3 d at 18 °C in bottles containing a square of Whatman filter paper (3.5 × 3.5 cm^2) soaked with 1 mL of a 10 mg ml^{-1} solution of pCPA (Sigma, C6506) in vehicle, or with 1 ml of vehicle alone. This treatment lasted 3 d, during which bottles were renewed after 1.5 d. For both CXM and pCPA treatments, drug feeding only occurred before conditioning. After massed or spaced conditioning, flies were kept in regular bottles with fresh medium for 24 h.

Immunohistochemistry. *NP0047-GAL4* flies were crossed with *UAS-mCD8::GFP* or *UAS-mCD8::GFP; Th-GAL80; UAS-mCD8::GFP* flies. The brains of female progeny were prepared 5–10 d after hatching at 25 °C by a standard immunolabeling procedure using antibodies to tyrosine hydroxylase (mouse, 1:200, Immunostar) and GFP (rabbit, 1:1,000, Invitrogen) and imaged with confocal microscopy (Olympus FV1000). Nomenclature of brain regions follows ref. 43.

***In vivo* calcium imaging.** Fly surgery and technical details of data acquisition were essentially performed as previously described[41]. Measurements were performed on 1–2-d-old female *w^{1118}/w^{1118}; UAS-GCaMP3/+; NP0047-GAL4/+* flies, except for imaging experiments on the *radish* (*rsh*) mutant, in which *w^{1118}/Y; UAS-GCaMP3/+; NP0047-GAL4/+* and *rsh/Y; UAS-GCaMP3/+; NP0047-GAL4/+* males were compared. For experiments on naive flies, flies were taken directly from crosses vials. For experiments on conditioned flies, a group of flies trained with octanol as negatively reinforced odorant, was collected immediately after the end of conditioning protocol in a food-containing vial and left for about 5 min. A fly was caught without anesthesia, then glued and operated essentially as previously described for *in vivo* imaging[41]. To eliminate motion artifacts that are detrimental to measurement of unprovoked fluorescence changes, the proboscis was glued to the thorax, and at the end of surgery the brain was covered with a 15-µl drop of *Drosophila* Ringer's solution[41] supplemented with 1% agarose. The recording chamber was then placed beneath the water-immersion 20× objective (NA = 1, Leica) of a TCS-SP5 laser-scanning confocal microscope (Leica), fluorescence thus being collected from transverse sections of the brain observed from the top. Laser power (488 nm) was adjusted to obtain similar levels of emission throughout experiments. We observed no systematic bias of the laser power for a specific type of conditioned flies. The average delivered light power, as measured below the objective, was 50 µW with an s.d. of 8 µW. Imaging experiments were performed at 20 °C. On a sample of experiments, we measured that the average temperature change of the liquid bathing the brain between the beginning and the end of experiment was 0.3 °C, with a maximum of 1.3 °C. Measurements before and after a single 7-min recording did not yield noticeable temperature change either (−0.09 ± 0.14 °C, n = 13).

For single-plane acquisitions, the frame rate was 1 frame every 413 ms. Whenever it was possible to confidently discriminate MV1 from MP1 neurons, simultaneous recordings of activity in both neurons were performed by dual-plane acquisition in two planes at least 20 µm distant from one another (**Fig. 3c**). We performed 6–7-min recordings with typically 3–4-min intervals, repeated for variable duration, typically 1 h, and sometimes up to 2 h. At the end of the experiment, spontaneous or brush tickling–evoked leg or abdomen movement was checked to ensure that the fly was still alive.

For imaging of thermal activation of MV1 and MP1 neurons (**Supplementary Fig. 5**), *w^{1118}/w^{1118}; UAS-GCaMP3, UAS-TrpA1/+; NP0047-GAL4/+* flies raised at 18 °C were prepared in the same way, but the agarose step was omitted because of thermal sensitivity of *TrpA1*. Two acquisitions were made, after which the imaging cell holding the fly was placed inside a 60 °C incubator until the temperature inside the cell reached 30 °C (3 to 3.5 min). The liquid bathing the brain was then immediately replaced with a fresh one at 20 °C, and the fly was put back under the microscope.

Image analysis was performed offline with a custom-written Matlab program. Light intensity was averaged over a region of interest delimited by hand and surrounding the projections of dopaminergic neurons on the mushroom bodies in the observed plane. Neuropils chosen as controls depended on the plane where the acquisition was performed; in planes in which MV1 and MP1 neurons were visible, control neuropils were labeled structures from the ellipsoid body. For acquisitions at the V1 neurons' depth, control neuropils were processes on the central region of the brain of unidentified origin, but not corresponding to dopaminergic neurons, as their labeling was not suppressed by *Th-GAL80*. From a given region of interest, the resulting time trace was normalized to a percent change of fluorescence (100 ($F - F_0$) / F_0), using a baseline value of the fluorescence F_0 that was estimated as the mean fluorescence over the whole acquisition. To remove long-term drift, a baseline resulting from the moving average over a 100-s time window was then subtracted from the signal. Thus, in subsequent frequency analyses, all frequency axes are presented starting at 0.01 Hz. Given that signals are noisy, their amplitudes were estimated as the difference between the means of the 30% upper and lower quantiles of data points. We checked that two other methods of calculation, one similar, but excluding the 5% upper and lower quantiles, as outliers and one using the r.m.s. value of the signal as a value of amplitude, yielded similar results (data not shown).

For each signal, the power spectrum was computed and smoothed over a frequency window of 0.02 Hz. Rhythmic spontaneous activity in the time domain resulted in a peak in the power spectrum that had a finite width, as oscillations are intrinsically noisy. A fit of a Lorentzian curve to the power spectrum was performed to yield an estimate of the central frequency of the peak, f_0, and the width of the peak at half its maximal value, Δf. f_0 defined the characteristic frequency of the oscillation and frequency fluctuations around f_0, and hence the regularity of the oscillation, could be quantified by the quality factor $Q = f_0/\Delta f$ (ref. 44). A quality factor greater than 0.5 indicates that the zero frequency is excluded from the peak: this value was thus taken as a threshold to define a signal as rhythmically oscillating. When the fitting procedure converged to a value below 0.5, it was thus irrelevant to define oscillating parameters, and f_0 and Q were both assigned zero values.

doi:10.1038/nn.3055

Only one hemisphere per fly was considered for calculation of averages. When both hemispheres were visible, which was generally the case, the brighter one was selected.

Some flies showed sparse oscillatory sequences lasting for only one or two recordings, whereas others were robustly oscillating throughout most or all of the experiment. As the flies were not all imaged for the same duration, we set the following criterion: flies were considered to be robustly oscillating if more than half of the recordings in MV1 and MP1 neurons were oscillatory.

For time course analyses of amplitude, frequency and quality factor, recordings were pooled according to their starting time after the end of the conditioning protocol (trained flies) or the start of the dissection (naive flies), in time intervals of 500 s. To plot average amplitude histograms, we calculated a mean amplitude value for MV1 and MP1 neurons, V1 neurons, and control neuropil for each fly, and then averaged the mean values across all flies from the same condition.

Average power spectra across all animals from the same condition were obtained from signals in the 40–55-min range after the end of conditioning (or the dissection start for naive flies) and were additionally smoothed over a 0.03-Hz frequency window. Peaked average spectra (**Figs. 4b** and **6b**) were characterized by their mean frequency f_0 and a quality factor Q calculated from f_0 and the width at half-height.

Statistical analyses. All average data are presented as mean ± s.e.m. To compare two series of data, we used two-tailed unpaired t tests, except in **Supplementary Figure 5b**,**c**, where paired t tests were applied to compare activity in single flies before and after thermal activation. To compare more than two groups, we used one-way ANOVA followed by pairwise planned comparisons between relevant groups with a Student-Newman-Keuls test. Comparisons of parallel time series, or of average spectra, between different conditions employed two-way balanced ANOVA.

ANOVA results are given as the value of the Fisher distribution $F_{x,y}$ obtained from the data, where x is the degrees of freedom for groups and y is the total degrees of freedom of the distribution. Statistical comparison of the proportion of robustly oscillating flies in two groups was made with a two-sided Fisher's exact test[45]. The P value presented is the one defined in the 'minimum likelihood' approach, as defined in this reference.

40. Pascual, A. & Préat, T. Localization of long-term memory within the *Drosophila* mushroom body. *Science* **294**, 1115–1117 (2001).
41. Séjourné, J. *et al.* Mushroom body efferent neurons responsible for aversive olfactory memory retrieval in *Drosophila*. *Nat. Neurosci.* **14**, 903–910 (2011).
42. Yu, D., Akalal, D.-B.G. & Davis, R.L. *Drosophila* α/β mushroom body neurons form a branch-specific, long-term cellular memory trace after spaced olfactory conditioning. *Neuron* **52**, 845–855 (2006).
43. Otsuna, H. & Ito, K. Systematic analysis of the visual projection neurons of *Drosophila melanogaster*. I. Lobula-specific pathways. *J. Comp. Neurol.* **497**, 928–958 (2006).
44. Plaçais, P.-Y., Balland, M., Guérin, T., Joanny, J.-F. & Martin, P. Spontaneous oscillations of a minimal actomyosin system under elastic loading. *Phys. Rev. Lett.* **103**, 158102 (2009).
45. Rivals, I., Personnaz, L., Taing, L. & Potier, M.-C. Enrichment or depletion of a GO category within a class of genes: which test? *Bioinformatics* **23**, 401–407 (2007).

Supplementary information

Slow oscillations in two pairs of dopaminergic neurons gate long-term memory formation in *Drosophila*

Pierre-Yves Plaçais[1,6], Séverine Trannoy[1,6], Guillaume Isabel[1,5,6], Yoshinori Aso[2,5], Igor Siwanowicz[2], Ghislain Belliart-Guérin[1], Philippe Vernier[3], Serge Birman[4], Hiromu Tanimoto[2] and Thomas Preat[1]

[1] Genes and Dynamics of Memory Systems, Neurobiology Unit, CNRS, ESPCI, Paris, France.

[2] Behavioral Genetics, Max Planck Institute of Neurobiology, Martinsried, Germany.

[3] Développement, Evolution, Plasticité du Système Nerveux, Institut de Neurobiologie Alfred-Fessard, CNRS, Gif-sur-Yvette, France.

[4] Genetics and Physiopathology of Neurotransmission, Neurobiology Unit, CNRS, ESPCI, Paris, France.

[5] Present addresses: Centre de Recherches sur la Cognition Animale, Université Paul Sabatier, Toulouse, France (G.I.); Janelia Farm Research Campus, HHMI, Ashburn, Virginia, USA (Y.A.).

[6] These authors contributed equally to this work.

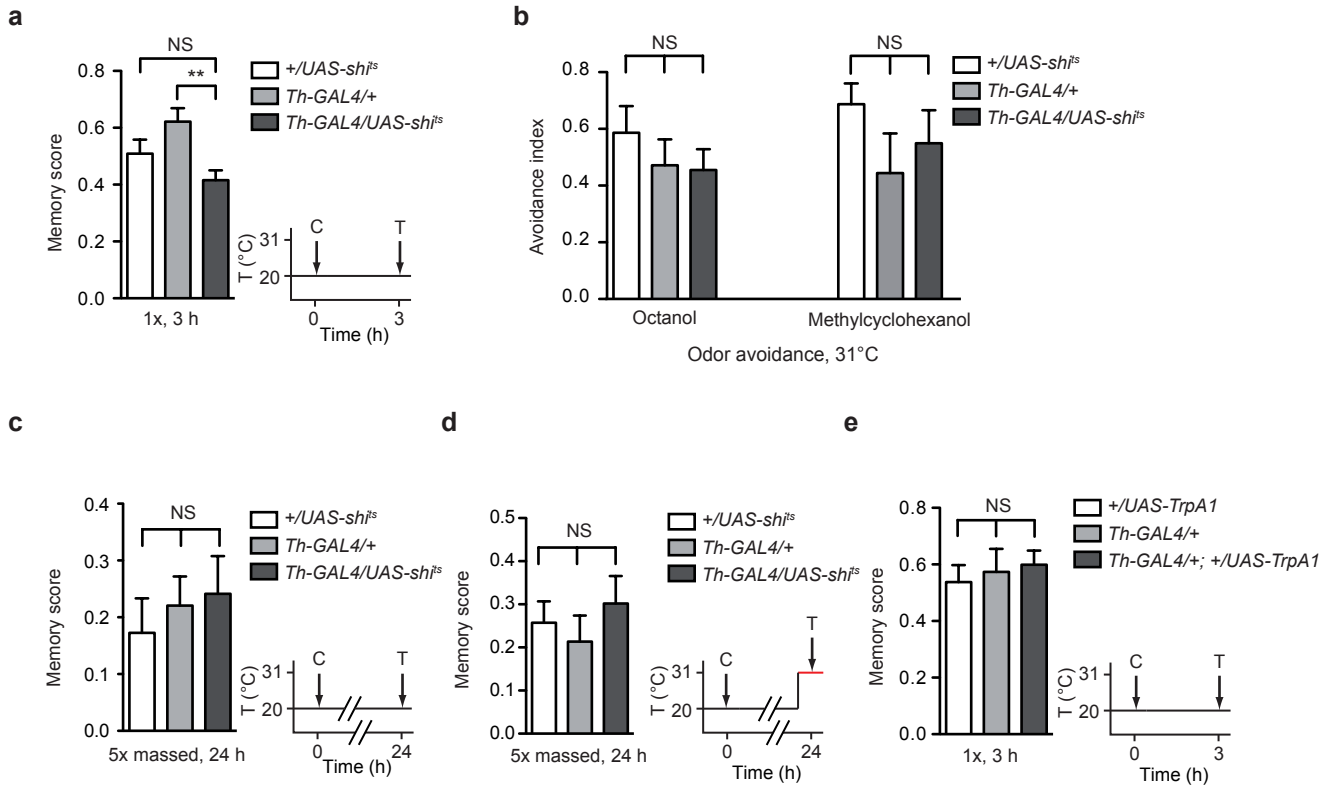

Supplementary Figure 1: Behavioral controls for experiments with *Th-GAL4*.
(**a**) *Th-GAL4/UAS-shi*^{ts} flies showed a normal 3 h performance at permissive temperature (20°C) after single cycle conditioning ($F_{(2,41)} = 5.350$, $p = 0.0086$, $n \geq 14$. *Post hoc* pairwise comparisons: *Th-GAL4/UAS-shi*^{ts} *vs. Th-GAL4/+*: $p < 0.01$, *Th-GAL4/UAS-shi*^{ts} *vs. +/UAS-shi*^{ts} : $p > 0.05$). (**b**) Olfactory acuity of *Th-GAL4/UAS-shi*^{ts} flies was similar to that of the genetic controls at restrictive temperature (31°C) both for 3-octanol (O; $F_{(2,21)} = 0.6754$, $p = 0.5197$, $n = 8$), and 4-methylcyclohexanol (M; $F_{(2,21)} = 1.156$, $p = 0.3340$, $n = 8$). (**c**) *Th-GAL4/UAS-shi*^{ts} flies showed a normal 24 h performance at permissive temperature (20°C) after massed conditioning ($F_{(2,35)} = 0.35$, $p = 0.71$, $n = 12$). (**d**) Blocking dopaminergic neurons output during memory retrieval after massed training did not alter 24-hour memory performance ($F_{(2,45)} = 0.5691$, $p = 0.54$, $n \geq 15$). (**e**) *Th-GAL4/+; +/UAS-TrpA1* flies showed a normal 3h performance at permissive temperature (20 °C) after single cycle conditioning ($F_{(2,21)} = 0.22$, $p = 0.802$, $n = 8$).

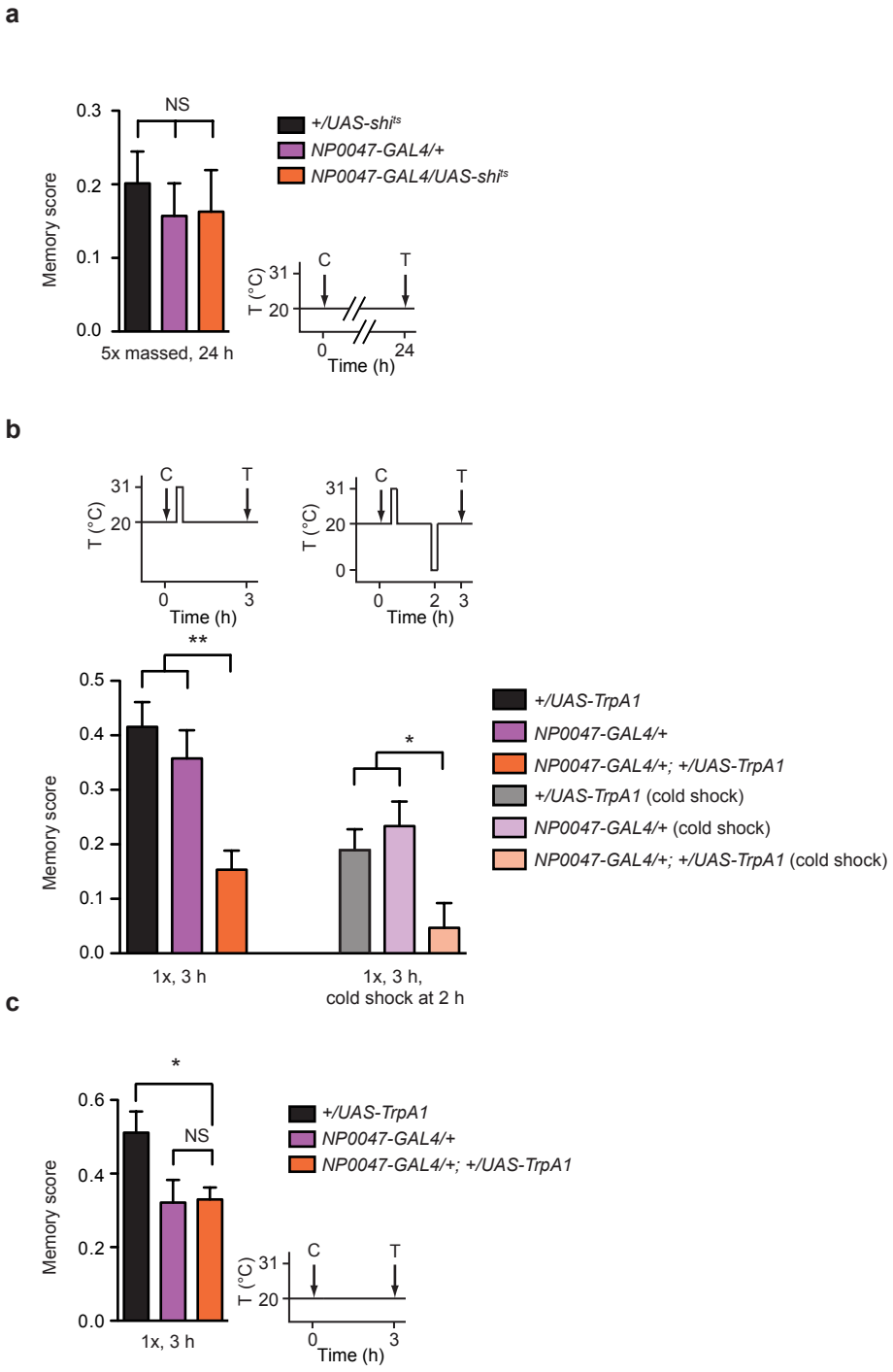

Supplementary Figure 2: Behavioral controls for experiments with *NP0047-GAL4* and cold shock experiment.

(**a**) *NP0047-GAL4/UAS-shi*^{ts} flies showed a normal 24 h performance at permissive temperature (20°C) after massed conditioning ($F_{(2,20)} = 0.25$, $p = 0.78$, $n = 7$). (**b**) One-minute activation of *NP0047-GAL4* neurons straight after single cycle conditioning impairs 3 h memory ($p = 0.0003$, $n \geq 14$). The memory drop persisted when a 2 min cold-shock anesthesia was performed 2 h after training ($p = 0.0084$, $n \geq 18$), showing that ARM is decreased. (**c**) *NP0047-GAL4/+; +/UAS-TrpA1* flies showed a normal 3 h performance at permissive temperature (20°C) after single cycle conditioning ($F_{(2,20)} = 4.27$, $p = 0.03$, $n = 7$. Post hoc pairwise comparisons: *NP0047-GAL4/+; +/UAS-TrpA1 vs. NP0047-GAL4/+*: $p > 0.05$, *NP0047-GAL4+; +/UAS-TrpA1 vs. +/UAS-TrpA1* : $p < 0.05$).

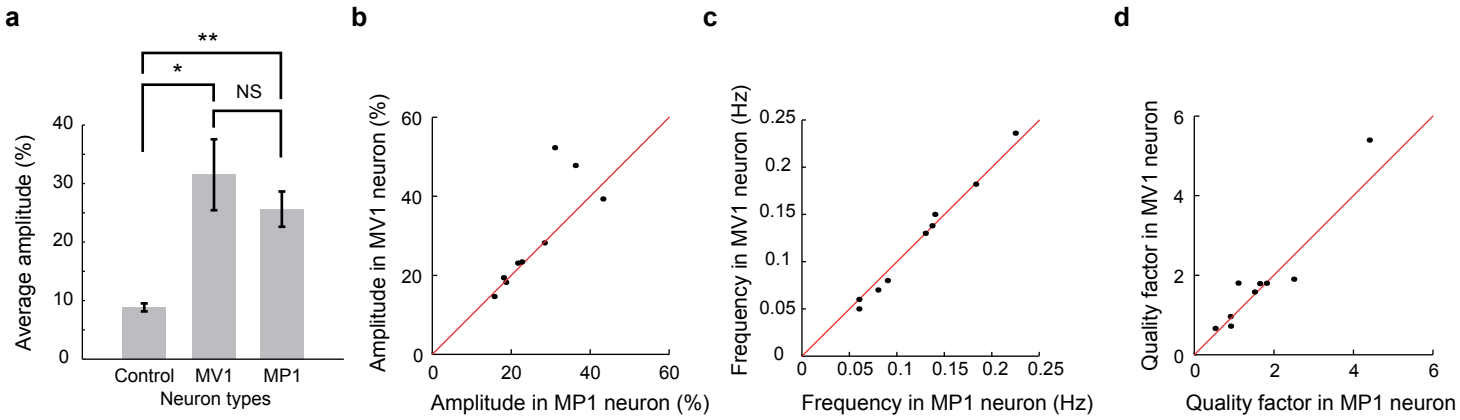

Supplementary Figure 3: Spontaneous activity in MV1 and MP1 neurons are indistinguishable. (**a**) Recordings were obtained for 6 flies at different times in regions where labeling could be unequivocally attributed to either MV1 or MP1 neurons. Both types of neurons show large amplitude spontaneous calcium changes compared with control structures ($p = 0.0028$, $n = 6$). (**b**–**d**): Correlation is high between signals from MV1 and MP1 neurons, considering amplitude (**b**) ($R^2 = 0.90$), frequency (**c**) ($R^2 = 0.99$) and quality factor (**d**) ($R^2 = 0.95$).

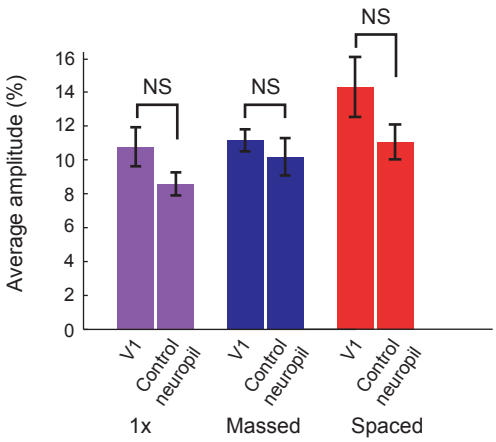

Supplementary Figure 4: No activity was detectable in V1 neurons after any type of conditioning. V1 neurons and neighbouring structures chosen as controls produced noisy signals of similar amplitude, after one cycle of conditioning ($p = 0.13$, $n = 8$ flies), five massed cycles ($p = 0.46$, $n = 11$) and five spaced cycles ($p = 0.08$, $n = 8$).

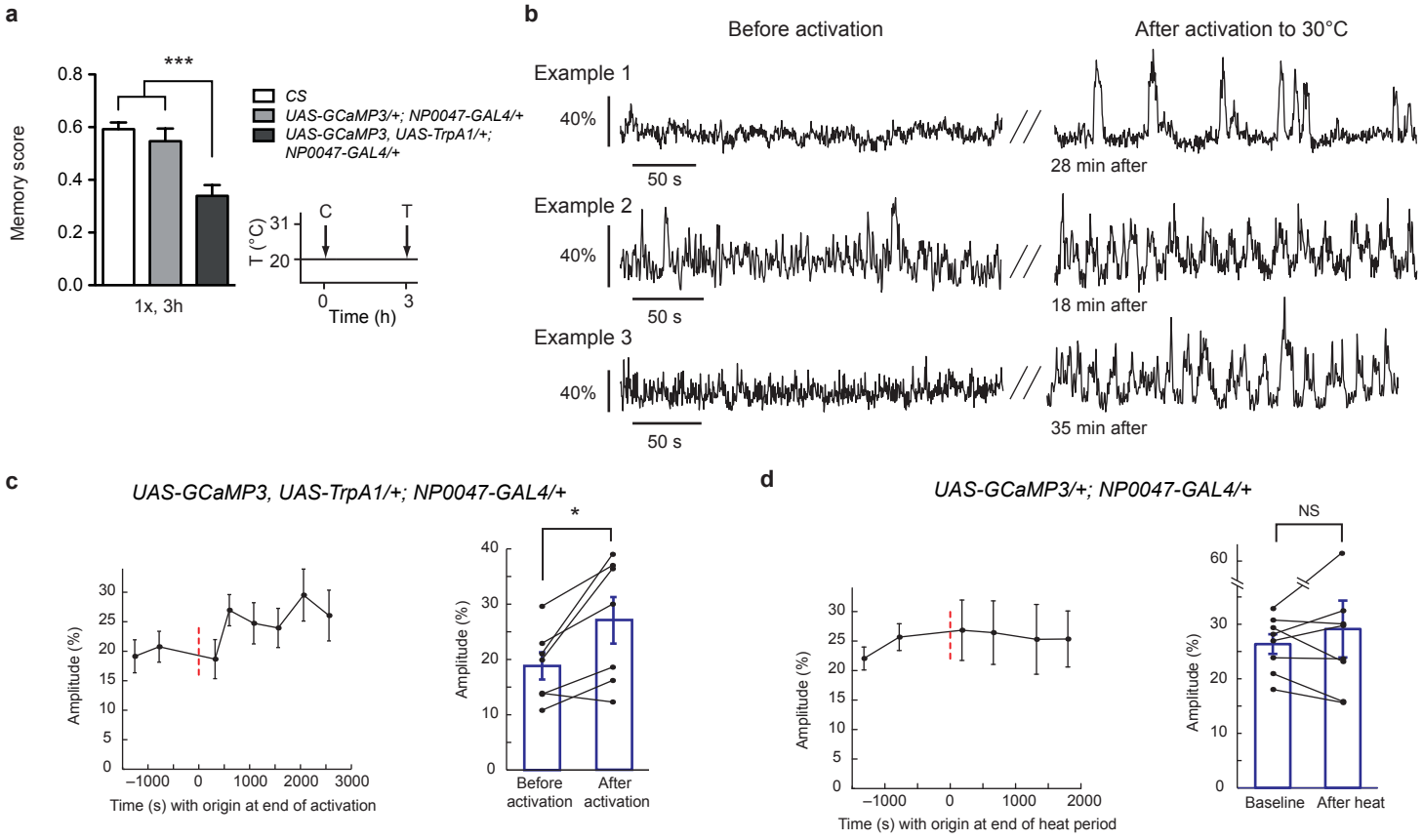

Supplementary Figure 5: Activity of MV1 and MP1 neurons is enhanced after *TrpA1* activation.
(**a**) Co-expression of *GCaMP3* and *TrpA1* in *NP0047-GAL4* neurons led to a defect in 3 h memory at permissive temperature ($F_{(2,20)} = 13.20$; $p < 0.0001$; $n \geq 9$). (**b**) From top to bottom, three examples illustrating the triggering of sustained, and sometimes oscillatory (bottom two examples), activity in MV1 and MP1 neurons by thermal activation in flies carrying *GCaMP3* and *TrpA1* with initially silent MV1 and MP1 neurons. (**c**) Time course of the long-lasting amplitude change in MV1 and MP1 neurons' activity triggered by a brief thermal activation to 30 °C, averaged over 7 flies (left). Plotting the maximal amplitude reached before and after activation reveals a significant increase (right, $p = 0.019$, paired t-test, $n = 7$). (**d**) By contrast, amplitude remained constant in flies not carrying *UAS-TrpA1*, and no significant increase could be measured ($p = 0.52$, paired t-test, $n = 8$). In this series of experiments in which agarose could not be applied on the brain to restrain its movement, baseline amplitude was higher than in other experiments. Thus baseline amplitude reached ~20% even in flies expressing both *GCaMP3* and *TrpA1*, whose MV1 and MP1 neurons had very little spontaneous activity.

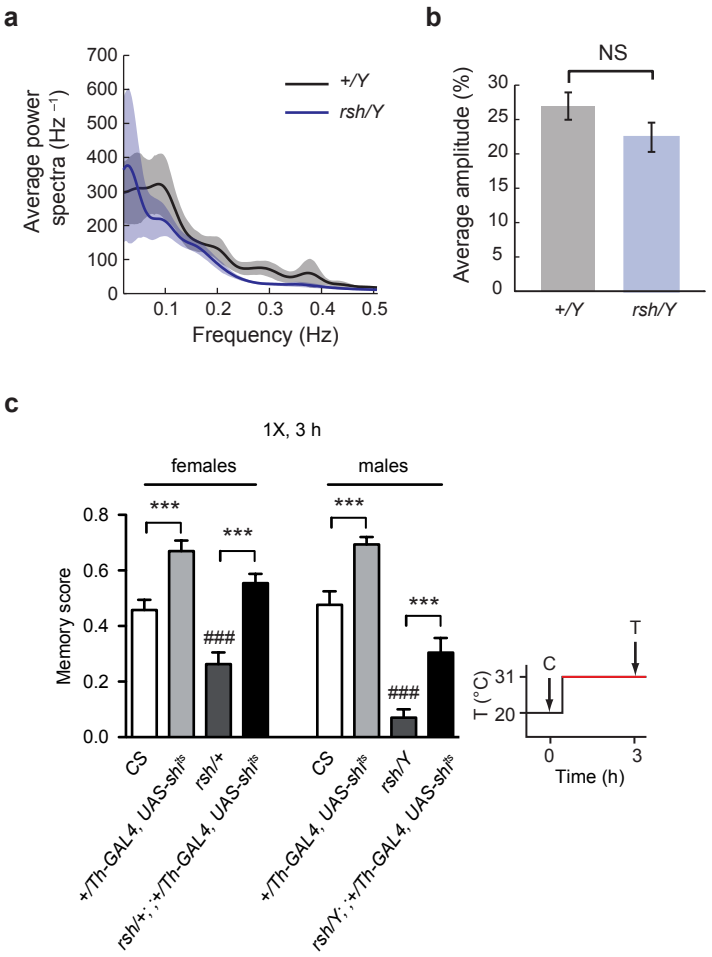

Supplementary Figure 6: Dopaminergic neurons' control over ARM levels is independent from the *radish* gene.

(**a**–**b**) Spontaneous activity of MV1 and MP1 neurons was similar in wild-type and *rsh* naive males. In both cases signals spanned a wide frequency range, resulting in monotonically decreasing power spectra (**a**) (*+/Y*: $n = 7$, 4 oscillating flies; *rsh/Y*: $n = 6$, 3 oscillating flies). The average amplitudes of MV1 and MP1 neurons' activity were also similar (**b**) ($p = 0.15$). (**c**) Consistent with imaging results, carrying the *radish* mutation did not prevent flies from forming additional memory when their dopaminergic neurons were blocked after conditioning (Females: $F_{(3,66)} = 20.59$; $p < 0.0001$; $n \geq 16$; Males: $F_{(3,62)} = 40.93$; $p < 0.0001$; $n \geq 15$; # symbols indicate the level of significance of the post-hoc test between *rsh/+* (respectively *rsh/Y*) and *CS*.

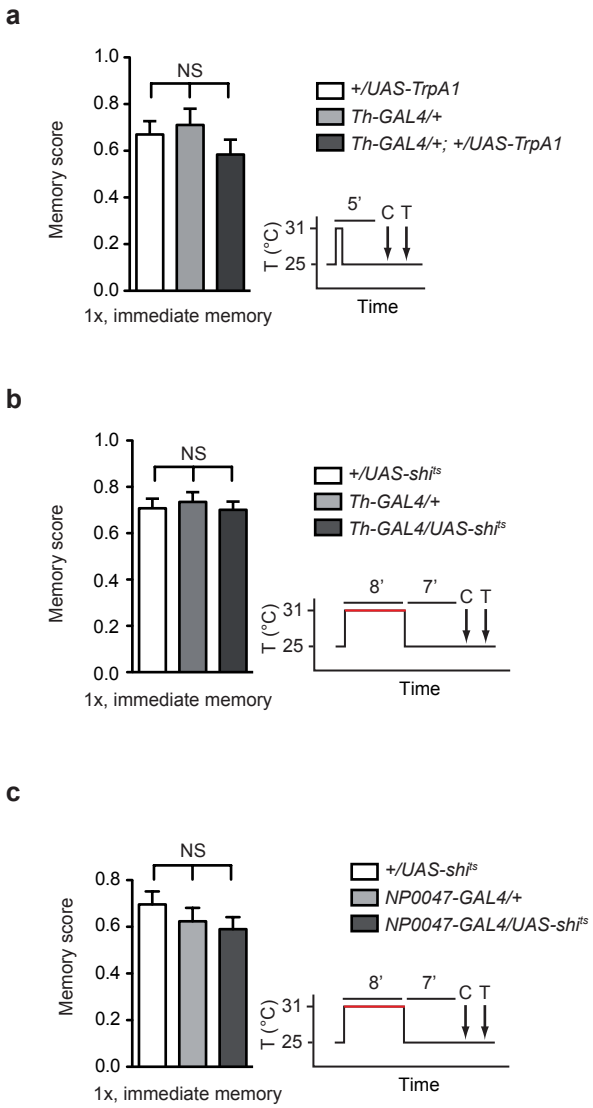

Supplementary Figure 7: Activation or blockade of dopaminergic neurons before single-cycle training does not impair learning.

(**a**) 1-minute activation of *Th-GAL4* neurons 5 minutes before single-cycle training did not impair learning [$F_{(2,29)} = 0.34$; $p = 0.37$; $n = 10$]. (**b**) 8-minute blockade of *Th-GAL4* neurons 15 minutes before single-cycle training had no effect on learning [$F_{(2,23)} = 0.20$; $p = 0.82$; $n = 8$]. (**c**) 8-minute blockade of *NP0047-GAL4* neurons 15 minutes before single-cycle training had no effect on learning [$F_{(2,23)} = 0.984$; $p = 0.39$; $n = 8$].

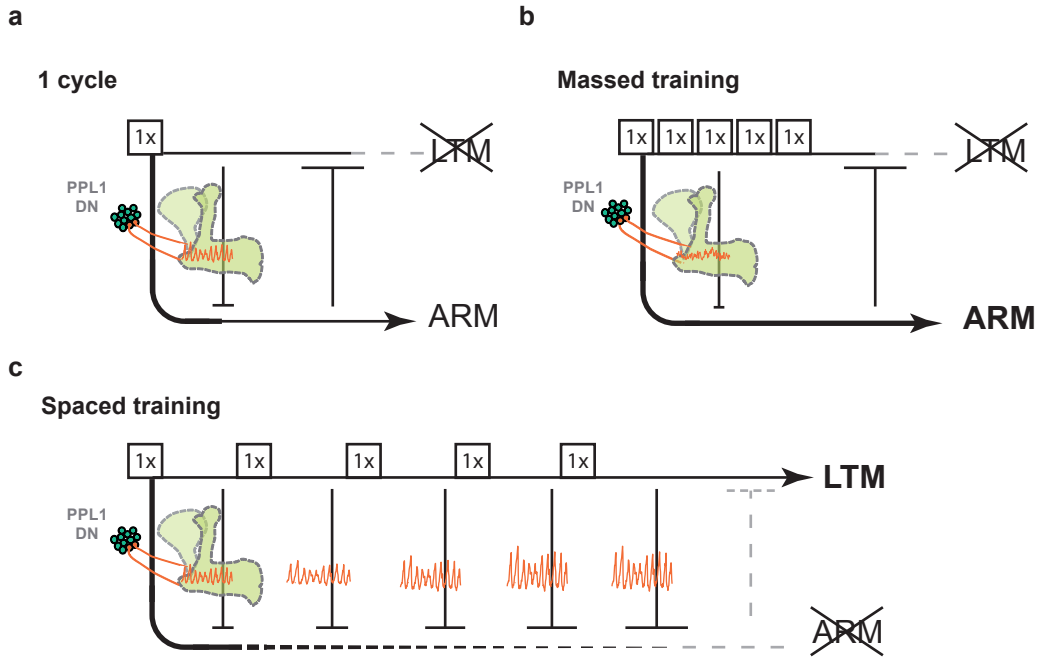

Supplementary Figure 8: ARM-regulating neurons gate LTM formation during the inter-trial intervals.

The three panels illustrate the role of oscillatory dopaminergic neurons after single cycle (**a**), massed (**b**) and spaced training (**c**), and their effect on the two independent pathways leading to the formation of consolidated ARM or LTM, respectively. (**a**) After single-cycle training, oscillatory modulation on the mushroom body from MV1 and MP1 neurons prevents excessive ARM formation and prepares the brain for a potential multiple and spaced experience, though sufficient activity of the ARM pathway remains which prevents LTM from being formed after this single cycle. (**b**) Massed training reduces the activity of MV1 and MP1 neurons, which leads to robust ARM consolidation and represses the LTM pathway. (**c**) Only during the rest intervals of a spaced training can oscillatory neurons repeatedly and fully inhibit ARM consolidation, letting the brain engage into the energetically costly LTM pathway[5].

Alternatively to this model, dopaminergic neurons oscillations could independently inhibit the ARM pathway and gate the LTM pathway, enabling the latter only when maintained all along spaced training.

Supplementary Movie 1: Confocal stack showing the *NP4700-GAL4* expression pattern visualized by *mCD8::GFP* (white). Neuropils are counterlabeled with an anti-synapsin antibody (orange).

Supplementary Movie 2: Confocal stack showing the *NP0047-GAL4* expression pattern visualized by *mCD8::GFP* (white). *TH* immunoreactive cells are labeled in magenta.

Supplementary Movie 3: Confocal stack showing the *NP0047-GAL4* expression pattern, in combination with *Th-GAL80*, visualized by *mCD8::GFP* (white). Neuropils are counterlabeled with an anti-synapsin antibody (orange).

Supplementary Movie 4: Confocal stack showing the *NP0047-GAL4* expression pattern, in combination with *Th-GAL80*, visualized by mCD8::GFP (white). *TH* immunoreactive cells are labeled in magenta.

Supplementary Movie 5: Spontaneous activity oscillations in MB projections from MV1 and MP1 neurons. This movie is accelerated 10 times; the real duration of the recording was 330 s. Oscillation characteristics were: left hemisphere: f_0 = 0.11 Hz, Q = 2.1, amplitude 29% and right hemisphere: f_0 = 0.105 Hz, Q = 1.6 amplitude 32%. Raw 8-bit grayscale images were smoothed with a 2-pixel radius Gaussian filter, a constant value of 30 was substracted from the resulting whole images, and contrast was then enhanced by rescaling intensity to reach 1.5% saturated pixels on one oscillation peak image (image processing performed with ImageJ).